IJPSR (2012), Vol. 3, Issue 08 **(Research Article)**

INTERNATIONAL JOURNAL OF PHARMACEUTICAL SCIENCES AND RESEARCH

Received on 02 April, 2012; received in revised form 21 June, 2012; accepted 29 July, 2012

OPTIMISATION OF TYROSINE-BASED LEAD MOLECULES CAPABLE OF MODULATION OF THE PEROXISOME PROLIFERATOR-ACTIVATED RECEPTOR GAMMA

J. Ciantar*[1], C. Shoemake [1], C. Mangani [2], L.M. Azzopardi [1] and A Serracino Inglott [1]

Pharmacy Department [1], Faculty of Medicine and Surgery, University of Malta, Msida MSD 2080, Malta
Chemistry Department [2], Faculty of Science, University of Malta, Msida 2080, Malta

Keywords:
Diabetes,
Drug design,
Farglitazar,
Peroxisome proliferator-activated receptor gamma,
Rosiglitazone,
Tyrosine agonists

Correspondence to Author:

J. Ciantar

Pharmacy Department, Faculty of Medicine and Surgery, University of Malta, Msida MSD 2080, Malta

E-mail: jcia0002@um.edu.mt

ABSTRACT

The peroxisome proliferator-activated receptor gamma (PPARγ) agonist rosiglitazone has recently been withdrawn from the European market and its use has been restricted in the US due to its undesirable effects which were considered to outweigh its benefits. Literature indicates that there are two agonist bound conformations of the PPARγ as exemplified by its binding to rosiglitazone (PDB ID; 1FM6) and to farglitazar (PDB ID; 1FM9). This study aims to explore these two conformations, and to evaluate whether they should be targeted separately in the context of drug design studies. Furthermore, it was aimed to design a series of molecules with the potential to act as leads in a drug design process and the capability of agonist activity at the PPARγ with an acceptable side effect profile. *In silico* ligand binding affinities (p*K*d) of rosiglitazone and farglitazar within their cognate receptors were 6.62 and 9.70 respectively. The farglitazar conformer that bound optimally within the rosiglitazone bound PPARγ ligand binding pocket was identified and its binding affinity (p*K*d) re-determined. An analogous conformational analysis of rosiglitazone within the farglitazar bound PPARγ ligand binding pocket was carried out. The binding affinities (p*K*d) for these optimum conformations were 8.12 and 6.16 respectively. *De novo* novel structures were generated *in silico* based on the tyrosine-agonist farglitazar and its cognate ligand binding pocket. Moreover, analysis of the binding modality of farglitazar indicates that this molecule accesses the PPARγ ligand binding pocket more completely than does rosiglitazone. Binding affinity studies have shown that the PPARγ ligand binding pocket adopts diverse ligand driven conformations.

INTRODUCTION: The recent advance in the development of new remedies for the treatment of type 2 diabetes mellitus is a result of the increase in the incidence of this disease, as well as the high percentage of associated co-morbidities and deaths [1]. The thiazolidinediones are peroxisome proliferator-activated receptor gamma (PPARγ) agonists which were designed to manage type 2 diabetes mellitus owing to their ability to improve insulin sensitivity through actions which are completely different from those of other oral hypoglycaemic drugs [2]. Unfortunately, these drugs have been associated with a number of undesirable effects including fluid retention, weight gain [3], and an increase in risk of myocardial infarction [4].

This resulted in rosiglitazone being withdrawn from the European market, and in its restricted use within the US [5]. The different clinical profiles observed when different thiazolidinediones were compared are indicative of the potential for continued innovation within this class of drugs [6].

The study investigates, through a *de novo* drug design approach, two different bound conformations of the PPARγ receptor, as exemplified by its binding to rosiglitazone and that to farglitazar. These dissimilar conformations are the result of amino acid side chains orienting themselves differently around different ligands within the same receptor [7]. This is particularly encouraging from a drug design perspective since the PPARγ ligand binding pocket (LBP) appears to be capable of accommodating structurally diverse molecules.

This signifies that it would be possible to identify novel structures with the ability to bind to, and potentially activate this receptor and achieve normo-glycaemic status among type 2 diabetics for an acceptable side-effect profile. Salam *et al.* (2008) [8] sought to exploit the crystallographic data describing the varied conformations of the PPARγ LBP by performing a virtual screening exercise using a previously constructed in-house natural product library in order to indentify novel molecules with known affinity for the PPARγ and promising *in vivo* bioavailability. The current study emulates that of Salam *et al.,* (2008) [8], but differs essentially in the adoption of a *de novo* based approach using the structure of the previously identified PPARγ agonist farglitazar.

Tyrosine-based PPARγ agonists, such as farglitazar, have shown potent glucose-lowering activity *in vivo*[9] and have therefore been chosen as the basis for development of novel high affinity molecules in this study.

Method: The two agonist- bound conformations for the PPARγ receptor described by Salam *et al*., (2008) [8], highlighting the existence of the different PPARγ LBP conformations, obtained from the Protein Data Bank (PDB) [10] were used as templates in this study. These were PDB ID 1FM6 [7], describing the *holo*- co-ordinates of the PPARγ bound to rosiglitazone, and PDB ID 1FM9 [7], describing the *holo*- co-ordinates of the PPARγ bound to farglitazar. PPARγ is naturally found dimerised with the retinoid X heterodimeric receptor (RXR) which endogenously binds retinoic acid [11]. The crystallographic deposition 1FM6 consists of two PPARγ/RXR dimers which are bound together to form a tetramer, whereas the crystallographic deposition 1FM9 appears as a single PPARγ/RXR dimer[7] (**Figure 1**).

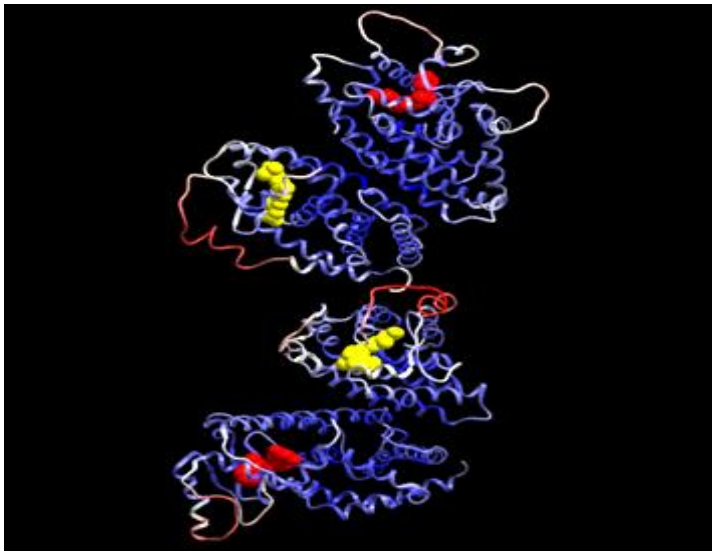

A

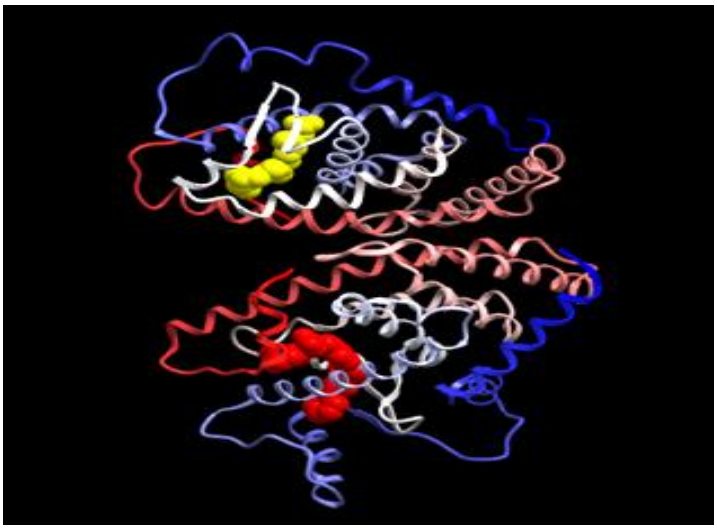

B

FIGURE 1: 1FM6 (A) AND 1FM9 (B) AS FOUND IN THE PDB; THE RXR RECEPTORS CAN BE SEEN BOUND TO RETINOIC ACID (YELLOW), AND THE PPARΓ RECEPTORS BOUND TO ROSIGLITAZONE (RED). Generated using Molsoft ICM Browser® [12].

The crystallographic depositions were read into Sybyl®[13] and simplified *in silico* in preparation for estimation of ligand binding affinity (LBA) (p*K*d). Simplification was performed in such a way that the bound coordinates of the ligand were retained and used as templates for further drug modeling. The simplification process included the;

1. Removal of water molecules owing to the fact that they were considered superfluous to ligand binding.

2. Removal of one dimer (in the case of 1FM6 which is found as a tetramer) and associated ligand.

3. Removal of the co-factors since it has been established that they do not alter ligand binding to the PPARγ.

4. Extraction of the bound small molecules rosiglitazone and farglitazar respectively in preparation for LBA (p*K*d) estimation.

The retinoic acid bound to the retained RXR moiety was not removed owing to the fact that literature indicates that retinoic acid causes a conformational change in the PPARγ moiety which alters LBA of the latter receptor for its cognate ligand [7].

The final outcome was a *holo* RXR receptor bound to the *apo* form of PPARγ for both crystallographic depositions. The bound co-ordinates of the small molecules rosiglitazone and farglitazar were saved separately. Estimation of binding affinities was carried out using the score algorithm [14].

High affinity conformers of farglitazar and rosiglitazone were then generated using the Similarity Suite in Sybyl® [13], which has the ability to generate viable binding conformations of potential ligands for an active site based on common 3D volume and proximity of important binding moieties. Farglitazar was therefore optimally docked into the rosiglitazone bound PPARγ LBP (1FM6) [7] and rosiglitazone into the farglitazar bound PPARγ LBP (1FM9) [7]. The result of this process was a preset number (n=21) of the highest affinity conformers for each ligand, output in a single *mol2* file, the contents of which were then individually visualized with ligand binding affinity (p*K*d) and energy being calculated in XScore® [14].

Rosiglitazone (the molecule co-crystallized with 1FM6) and the highest binding affinity (p*K*d) conformer of farglitazar were both used as probes in order to generate 3D maps and pharmacophores of the rosiglitazone bound PPARγ LBP (1FM6). These were then compared in order to determine and evaluate the extent of any differences between the two. LBP mapping and general pharmacophore identification was carried out in LigBuilder® [16], a program that designs small molecules *de novo* within the constraints of a pre-defined binding pocket. The first module of LigBuilder® [16], namely Pocket, was used in this part of the study.

The next part of the study was carried out in order to design novel molecules with antidiabetic properties and a more acceptable side-effect profile, which do not fall under the glitazone class. Molecular modeling was carried out using Sybyl® [13] and *de novo* design was executed using LigBuilder [16]. The seed was essentially the tyrosine moiety in farglitazar which was planted into the farglitazar bound PPARγ LBP at a locus analogous to that which it would have occupied had the farglitazar molecule itself been docked [17] (**Figure 2**).

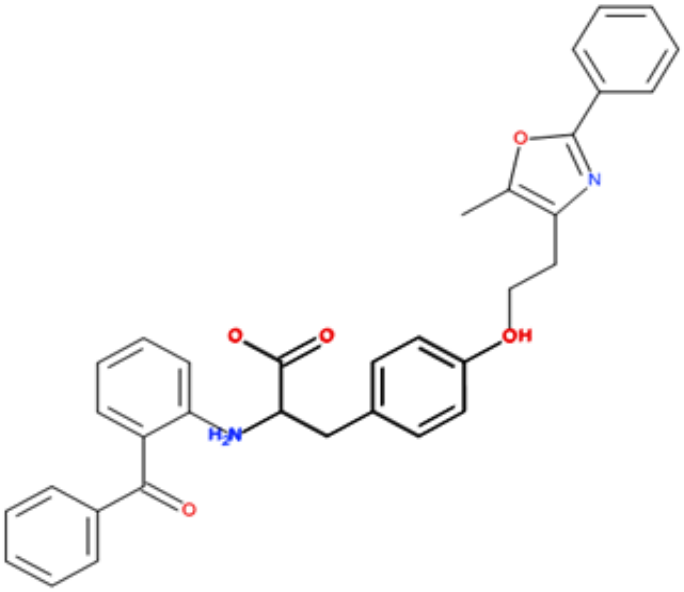

FIGURE 2: STRUCTURE OF FARGLITAZAR WITH ITS TYROSINE BACKBONE HIGHLIGHTED. Drawn using Accelrys Draw 4.0 ® [15].

Growing sites were then established through atom type assignation in which the atom type *H.spc* was recognizable to the Grow algorithm in LigBuilder®[16] as a site on which fragment attachment could occur. Two seeds were used for this study.

Both seeds had two potential growing sites, the first, that on the hydroxyl hydrogen attached to the benzene ring which was common to both. The difference lay in which of the two amine hydrogens was allowed growth as depicted in **Figure 3** below.

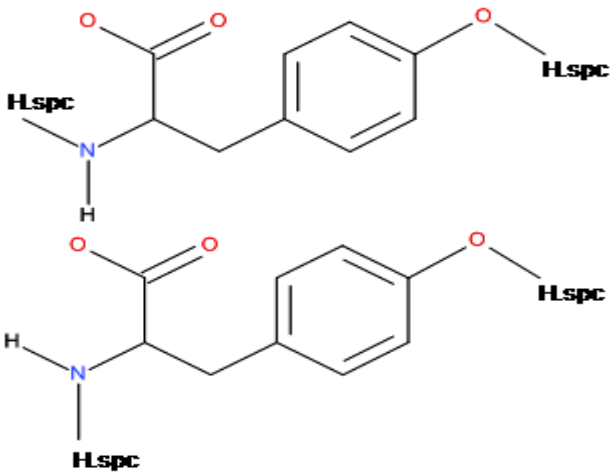

FIGURE 3: TYROSINE BACKBONE OF FARGLITAZAR CREATED AS SEED; SEED A (TOP), SEED B (BOTTOM). Drawn using Accelrys Draw 4.0® [15].

The result of this process was a number of analog families which were ranked according to predicted binding affinity (p*K*d) and bioavailability. The highest rankers in each family were chosen based on Lipinski's Rule of 5 [18] and were narrowed down on the basis of compliance with the Rule of 3 [19, 20]. The 82 highest rankers were then further reduced based on binding affinity (p*K*d).

RESULTS: The binding affinity (p*K*d) of rosiglitazone with its cognate receptor (1FM6) was 6.62 and that of farglitazar with its cognate receptor (1FM9) was 9.70. Twenty-one viable binding conformations of each ligand within its alternate receptor conformation were generated. The best binding conformer of farglitazar for the rosiglitazone bound LBP (1FM6) had a binding affinity (p*K*d) of 8.12 and the best binding conformer of rosiglitazone for the farglitazar bound LBP (1FM9) was 6.16 (**Table 1**).

TABLE 1: BEST BINDING CONFORMERS OF FARGLITAZAR AND ROSIGLITAZONE FOR THE ALTERNATE RECEPTORS. STRUCTURAL IMAGES GENERATED USING MOLSOFT ICM BROWSER® [12].

	Best binding conformer of farglitazar within PPARγ LBP 1FM6	Best binding conformer of rosiglitazone within PPARγ LBP 1FM9
Structure	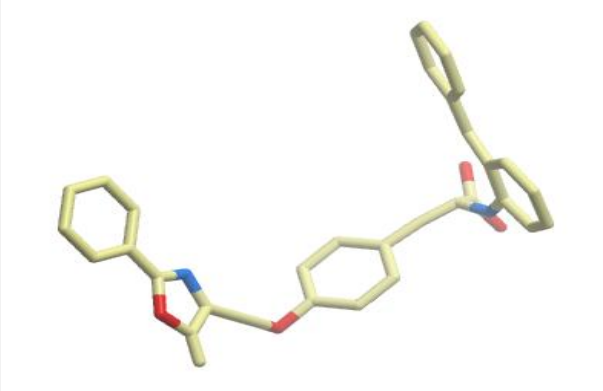	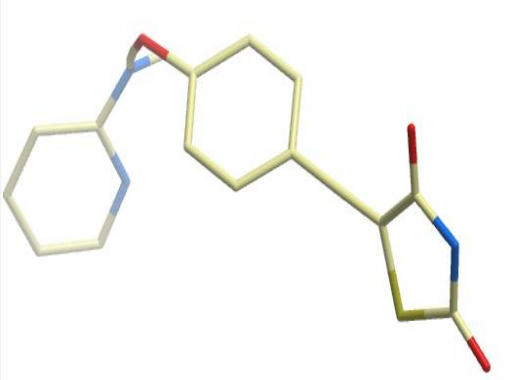
LBA (p*K*d)	8.12	6.16

Figure 4 shows the LBA (p*K*d) and binding energy (kcalmol^{-1}) for the 21 highest affinity conformers of rosiglitazone that were generated within the farglitazar bound PPARγ. The conformation with the greatest LBA (p*K*d=6.16) is shown in red.

Similarly, the LBA (p*K*d) and binding energy (kcalmol^{-1}) for the 21 highest affinity conformers of farglitazar that were generated within the rosiglitazone bound PPARγ can be seen in **Figure 5** below. The conformation with the greatest LBA (p*K*d=8.12) is shown in red.

Table 2 shows the *in silico* LBAs (p*K*d) of rosiglitazone and farglitazar bound to their cognate receptors compared with the LBAs (p*K*d) of their optimum conformers bound to the alternative receptor conformation.

The visual outputs of the mapped LBP's can be seen in **Figures 6 and 7**.

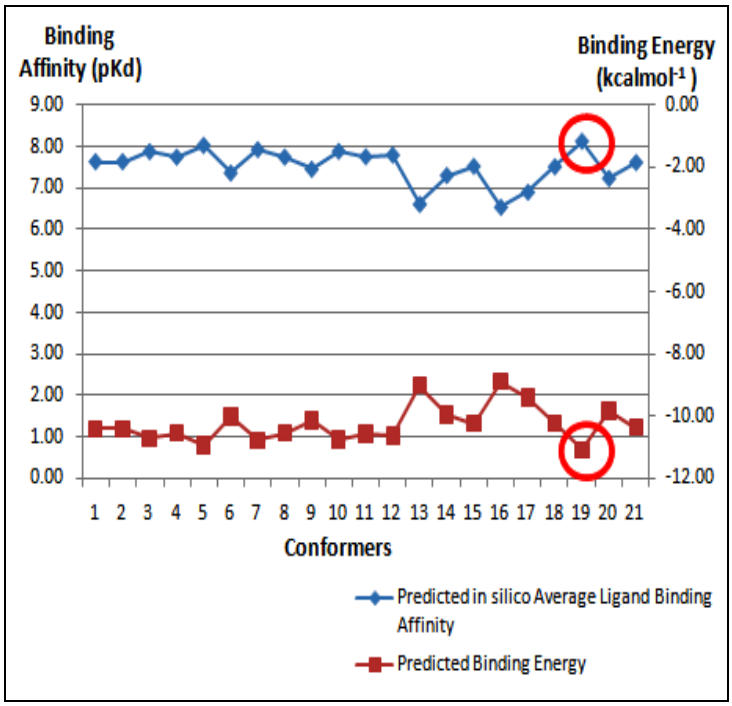

FIGURE 4: GRAPH OF BINDING AFFINITY (p*kd)/BINDING ENERGY* (kcalmol^{-1}) FOR THE 21 CONFORMATIONS OF FARGLITAZAR FOR THE ALTERNATE PPARγ LBP (1FM6)

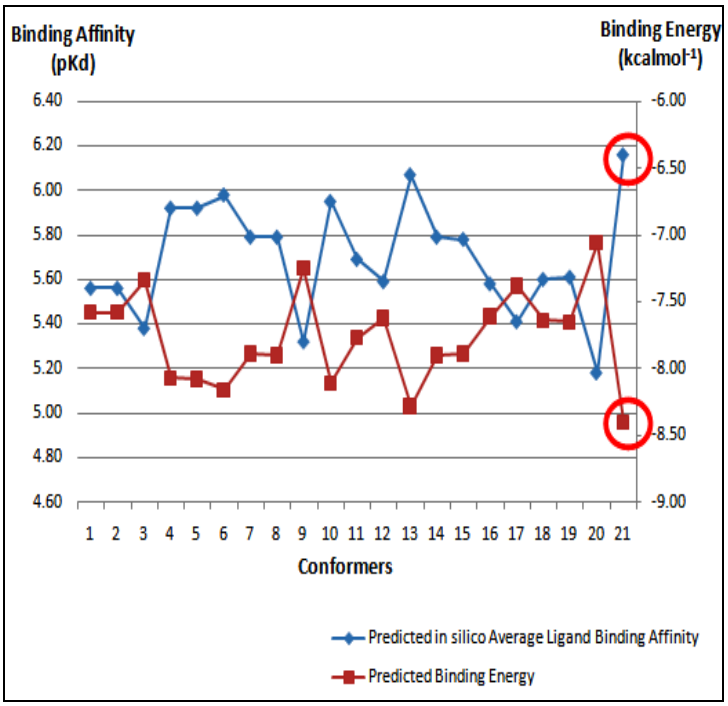

FIGURE 5: GRAPH OF BINDING AFFINITY (p*Kd)/Binding Energy* (kcalmol^{-1}) FOR THE 21 CONFORMATIONS OF ROSIGLITAZONE FOR THE ALTERNATE PPARγ LBP (1FM9)

TABLE 2: THE *IN SILICO* LBA (p*K*d) OF ROSIGLITAZONE AND FARGLITAZAR FOR THEIR COGNATE PPARγ RECEPTORS COMPARED WITH THE *IN SILICO* LBA (p*K*d) OF THE HIGHEST AFFINITY CONFORMERS FOR THE ALTERNATIVE PPARγ RECEPTORS

Rosiglitazone (Cognate Receptor 1FM6)		Farglitazar (Cognate Receptor 1FM9)	
LBA for its cognate receptor; 1FM6 (p*K*d)	**6.62**	LBA for its cognate receptor; 1FM9 (p*K*d)	**9.70**
LBA of conformer 021 for the alternative receptor; 1FM9 (p*K*d)	**6.16**	LBA of conformer 019 for the alternative receptor; 1FM6 (p*K*d)	**8.12**

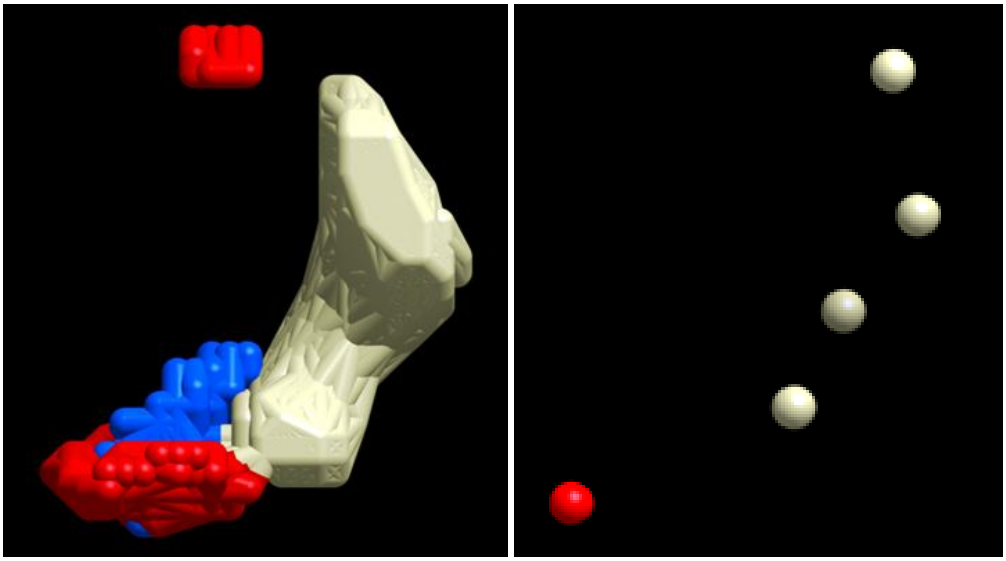

FIGURE 6: THE LBP OF THE ROSIGLITAZONE BOUND PPARγ AS DESCRIBED IN PDB ID: 1FM6 (LEFT) AND ITS RESPECTIVE PHARMACOPHORE (RIGHT). HYDROGEN BOND DONOR GRIDS ARE COLOURED IN BLUE, HYDROGEN BOND ACCEPTOR GRIDS IN RED AND HYDROPHOBIC GRIDS IN WHITE. Images generated using Molsoft ICM Browser® [12].

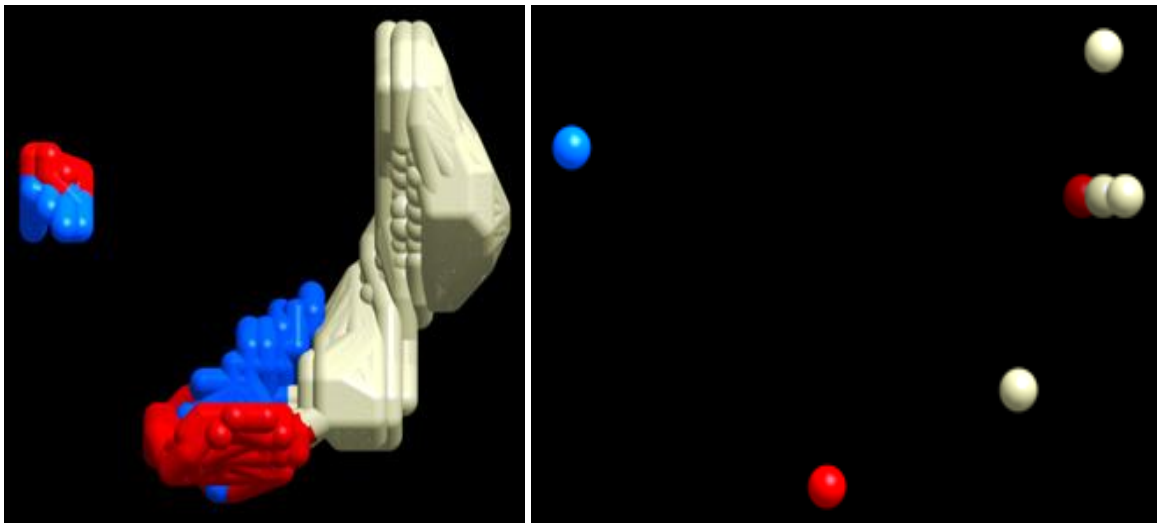

FIGURE 7: THE LBP OF THE FARGLITAZAR BOUND PPARΓ AS DESCRIBED IN PDB ID: 1FM6 (LEFT), AND ITS RESPECTIVE PHARMACOPHORE (RIGHT). FARGLITAZAR HERE IS NOT NATIVE (ROSIGLITAZONE) TO THE DESCRIBED CONFORMATION OF THE PPARγ LBP. HYDROGEN BOND DONOR GRIDS ARE COLORED IN BLUE, HYDROGEN BOND ACCEPTOR GRIDS IN RED AND HYDROPHOBIC GRIDS IN WHITE. Images generated using Molsoft ICM Browser® [12].

Multiple families of compounds were generated for each of the seeds all containing potential lead compounds for the PPARγ receptor. Twenty-seven highest rankers for seed A and 55 for seed B were identified and selected. None of the generated molecules fell within the Rule of 3 criteria [19]. The Rule of 3 [19] is a more stringent application of Lipinski's Rule of 5 [18] which is typically adhered to during lead molecule selection owing to the fact that it provides the leeway for structural alterations that are carried out during iterative optimization rounds that would consequently result in Rule of 5 [18] compliant end product molecules. Out of the selected molecules, 18 ligands were chosen as potential ligands for a novel drug design study – 2 resulting from seed A, and 16 from seed B (**Tables 3 and 4**).

TABLE 3: HIGHEST RANKERS OF EACH FAMILY FOR SEED A. Structural images and IUPAC names were generated using; Molsoft ICM Browser®[12], Accelrys Draw 4.0® [15], and Virtual Computational Chemistry Laboratory® [21].

IUPAC Name	Binding Affinity (p*K*d)	
(3Z,5E)-6-[2-[4-[(2S)-2-[[(4Z)-5-ethylhepta-4,6-dienyl]amino]-3,3-dihydroxy-propyl]phenyl]ethyl]-4-[(E)-3-hydroxyprop-1-enyl]octa-3,5,7-trienal	9.92	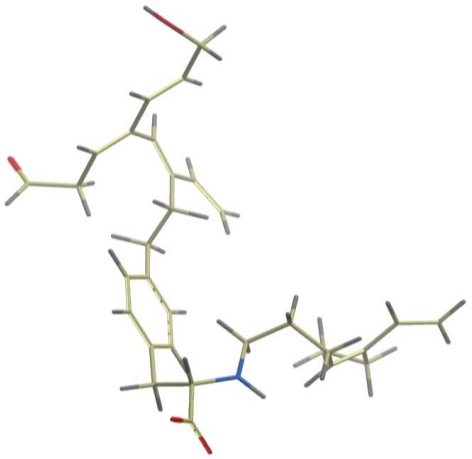

(2E,4E,6E,8R)-4-allyl-6-ethyl-8-[4-[(2S)-2-[[(3R)-3-ethylhexyl]amino]-3,3-dihydroxy-propyl]phenyl]octa-2,4,6-triene-1,1,8-triol	9.95	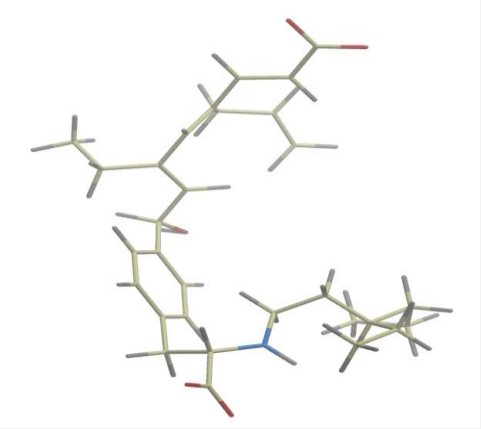

TABLE 4: HIGHEST RANKERS OF EACH FAMILY FOR SEED B. Structural images and IUPAC names were generated using; Molsoft ICM Browser®[12], Accelrys Draw 4.0®[15], and Virtual Computational Chemistry Laboratory® [21].

IUPAC Name	Binding Affinity (p*K*d)	Structure
(2R)-5-[(2S)-2-amino-3,3-dihydroxy-propyl]-N-[(3E,5E)-6-[(1R,3S)-3-ethylcyclopentyl]deca-3,5-dienyl]indane-2-carboxamide	9.15	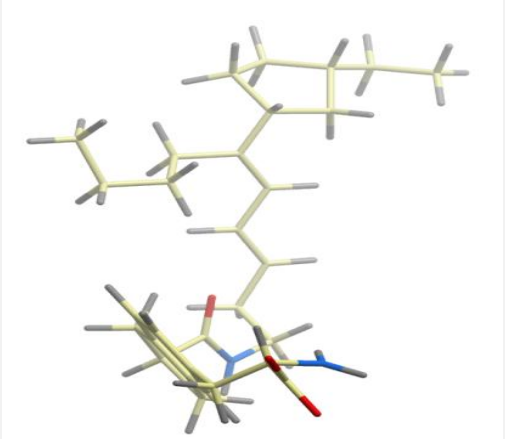
(2R)-N-[(3E)-3-[(5R)-5-[(3aS,7aS)-2,3,3a,6,7,7a-hexahydro-1H-inden-5-yl]cyclohex-2-en-1-ylidene]propyl]-5-[(2S)-2-amino-3,3-dihydroxy-propyl]indane-2-carboxamide; (2R)-5-[(2S)-2-amino-3,3-dihydroxy-propyl]-N-[(3E,5E)-6-[(1R,3S)-3-ethylcyclopentyl]deca-3,5-dienyl]indane-2-carboxamide	8.16	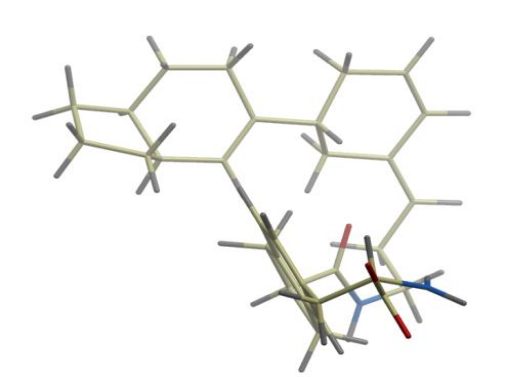
(2R)-5-[(2S)-2-amino-3,3-dihydroxy-propyl]-N-[(3E)-4-(1-methyl-2H-quinolin-6-yl)octa-3,7-dienyl]indane-2-carboxamide	7.57	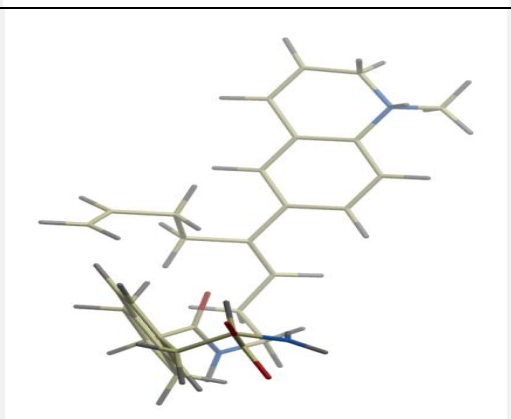

(2R)-5-[(2S)-2-amino-3,3-dihydroxy-propyl]-N-[(E)-4-[(3S,4S)-4-ethyl-3-methyl-cyclohexen-1-yl]but-3-enyl]indane-2-carboxamide	7.99	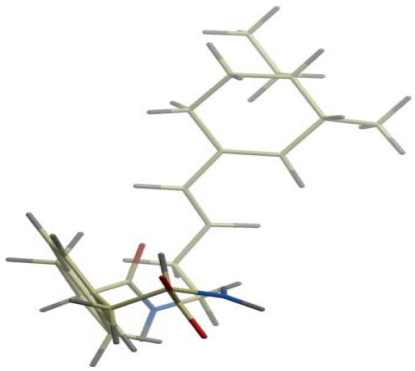
(2R)-5-[(2S)-2-amino-3,3-dihydroxy-propyl]-N-[(3Z,5E)-4-[(Z)-1-cyclopentylprop-1-enyl]-6-methyl-octa-3,5-dienyl]indane-2-carboxamide	7.91	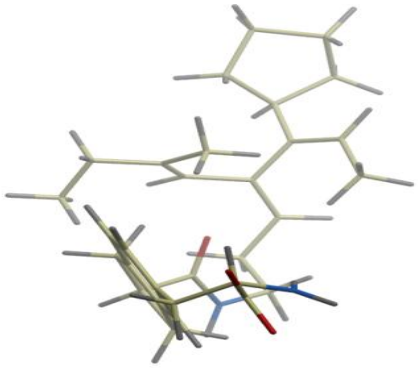
(2R)-5-[(2S)-2-amino-3,3-dihydroxy-propyl]-N-[(3Z,5E)-4-[(Z)-1-cyclopentylprop-1-enyl]-6-methyl-octa-3,5-dienyl]indane-2-carboxamide; (2R)-5-[(2S)-2-amino-3,3-dihydroxy-propyl]-N-[(3E,5E)-6-[(1S,2S)-2-isopropenylcyclopent-3-en-1-yl]nona-3,5-dienyl]indane-2-carboxamide	8.07	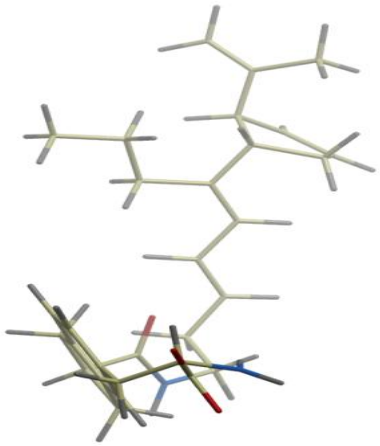
(2R)-5-[(2S)-2-amino-3,3-dihydroxy-propyl]-N-[(3E,5E)-6-[(1S,2S)-2-isopropenylcyclopent-3-en-1-yl]nona-3,5-dienyl]indane-2-carboxamide	8.07	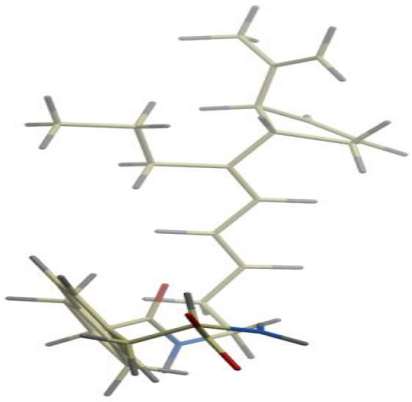

(2R)-5-[(2S)-2-amino-3,3-dihydroxy-propyl]-N-[(3E,5E)-6-[(1S,2S)-2-isopropenylcyclopent-3-en-1-yl]nona-3,5-dienyl]indane-2-carboxamide; (2R)-5-[(2S)-2-amino-3,3-dihydroxy-propyl]-N-[(3E)-3-[(1R)-1-vinyl-2,4-dihydro-1H-phenanthren-3-ylidene]propyl]indane-2-carboxamide	7.53	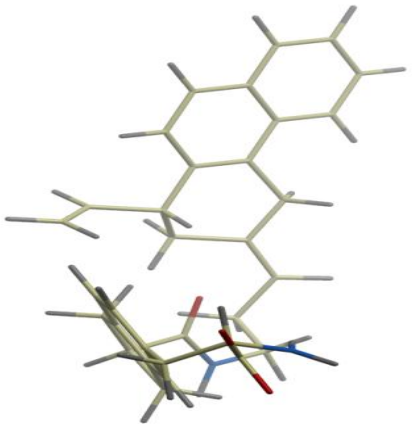
(2R)-5-[(2S)-2-amino-3,3-dihydroxy-propyl]-N-[(3E)-3-[(2R,3S,5R)-2-[(1Z)-hepta-1,6-dienyl]-3,5-dimethyl-cyclohexylidene]propyl]indane-2-carboxamide	7.98	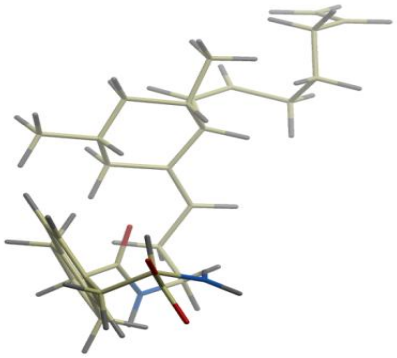
(2R)-5-[(2S)-2-amino-3,3-dihydroxy-propyl]-N-[(E)-4-(1-vinyl-2-naphthyl)but-3-enyl]indane-2-carboxamide	8.31	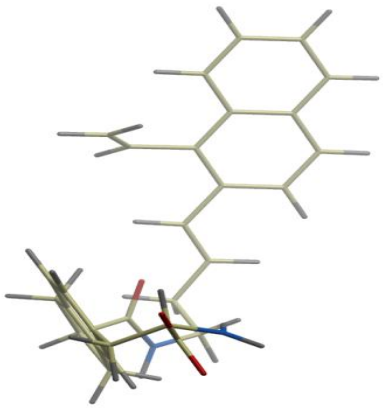
(2R)-5-[(2S)-2-amino-3,3-dihydroxy-propyl]-N-[(Z,9S)-9-[(1S)-cyclopent-2-en-1-yl]dec-2-enyl]indane-2-carboxamide	8.86	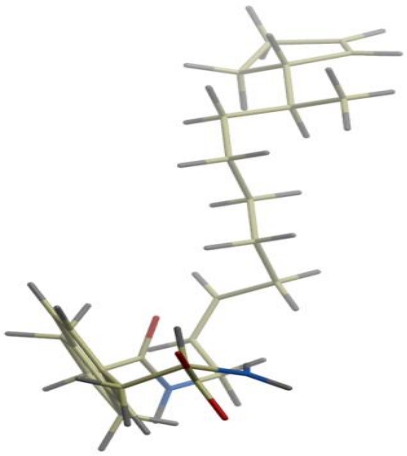

(2R)-5-[(2S)-2-amino-3,3-dihydroxy-propyl]-N-[(E)-4-[(4R,6S)-4-[(1S)-cyclohex-2-en-1-yl]-4,6-dimethyl-cyclohexen-1-yl]but-3-enyl]indane-2-carboxamide; (2R)-5-[(2S)-2-amino-3,3-dihydroxy-propyl]-N-[(Z,9S)-9-[(1S)-cyclopent-2-en-1-yl]dec-2-enyl]indane-2-carboxamide	8.66	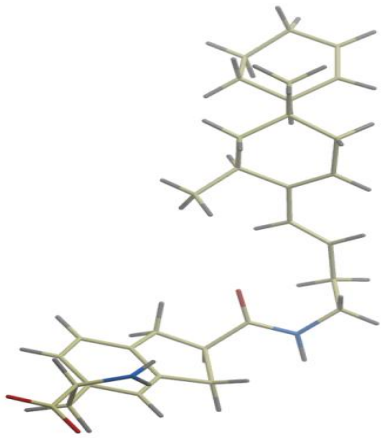
(2R)-5-[(2S)-2-amino-3,3-dihydroxy-propyl]-N-[(Z)-7-[(1S,5S)-5-ethylcyclopent-2-en-1-yl]hept-2-enyl]indane-2-carboxamide	8.02	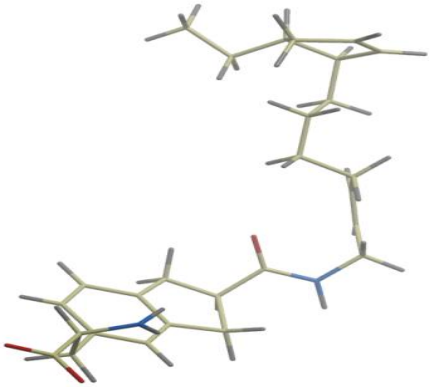
(2R)-5-[(2S)-2-amino-3,3-dihydroxy-propyl]-N-[(1S)-4-[(1R,5S)-5-[(1R)-cyclopent-2-en-1-yl]-2-ethyl-cyclohex-2-en-1-yl]-1-methyl-butyl]indane-2-carboxamide; (2R)-5-[(2S)-2-amino-3,3-dihydroxy-propyl]-N-[(Z)-7-[(1S,5S)-5-ethylcyclopent-2-en-1-yl]hept-2-enyl]indane-2-carboxamide	7.89	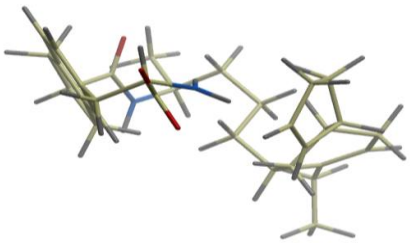
(2R)-5-[(2S)-2-amino-3,3-dihydroxy-propyl]-N-[2-[(1S,4R,5S)-5-cyclohexyl-4-methyl-cyclopent-2-en-1-yl]ethyl]indane-2-carboxamide	7.44	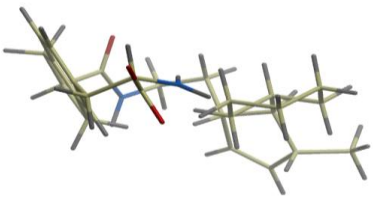
(2R)-5-[(2S)-2-amino-3,3-dihydroxy-propyl]-N-[2-[(1S,4R,5S)-5-cyclohexyl-4-methyl-cyclopent-2-en-1-yl]ethyl]indane-2-carboxamide; (2R)-5-[(2S)-2-amino-3,3-dihydroxy-propyl]-N-[(2Z,5E,7E)-5-[(Z)-3-(m-tolyl)prop-1-enyl]nona-2,5,7-trienyl]indane-2-carboxamide	7.43	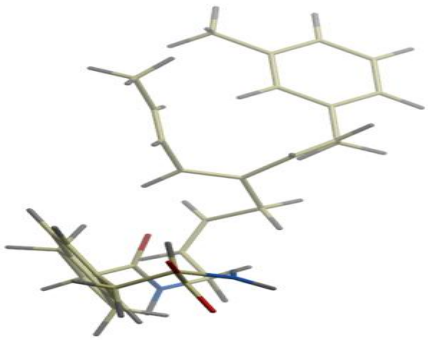

DISCUSSION: This study specifically aimed to demonstrate that the LBP of PPARγ adopted distinct conformations which were ligand driven – specifically one distinct conformation being adopted when PPARγ was bound to rosiglitazone (PDB ID; 1FM6) and another being adopted when PPARγ was bound to farglitazar (PDB ID; 1FM9). In addition, it sought to propose viable alternatives to the currently available thiazolidinediones, owing to the fact that their flagship molecule rosiglitazone while being recognised for its superior hypoglycaemic and dyslipidaemic effects has had its use completely withdrawn or restricted [5] due to its unacceptable side effect profile [3, 4].

Binding affinities decreased when rosiglitazone and farglitazar were bound to the alternate receptor conformations, in comparison with the binding affinities measured for these two ligands with their cognate receptor conformations. An interesting observation is that the lower affinity of rosiglitazone and the higher affinity of farglitazar appear to be preserved in the cognate and alternative conformations of the PPARγ LBP in each case.

Rosiglitazone with preserved bound co-ordinates, has a predicted *in silico* affinity of p*K*d 6.62 for its cognate receptor. This changed to p*K*d 6.16 when the highest affinity conformer for the farglitazar bound conformation of the PPARγ receptor was calculated. Similarly, farglitazar, with preserved bound co-ordinates was calculated to have a predicted *in silico* affinity (p*K*d) of 9.7 which decreased to 8.12 when the LBA (p*K*d) of the highest affinity conformer for the rosiglitazone bound conformation of the PPARγ receptor was calculated. The implications of this part of the study consequently are that;

- The receptors are in fact different and may be used as separate targets in a drug design project.
- The structural conformations of the highest affinity ligands of rosiglitazone and farglitazar for their alternative receptor conformations were identified, and could be put forward as templates for rigidification in bioisosteric exercises.

Mapping of the PPARγ LBP and generating proposed pharmacophoric structures using rosiglitazone bound to its cognate receptor conformation (1FM6) and the best affinity conformer of farglitazar bound with the rosiglitazone bound LBP (1FM6) was carried out in order to further support the notion that the PPARγ adopts distinct conformations which are ligand driven and dependant.

In fact, two different LBP maps were obtained and similarly, the predicted pharmacophores are not identical. Given that the receptor conformation being assessed is the same (1FM6) and that the variable is only the ligand, we conclude that the ligands are accessing the LBP at different levels.

This is understandable when we take into account the fact that 2°, 3° and 4° structures of a protein are a consequence of the hydrophobic effect which is the tendency of a protein to expose its hydrophilic residues to the external environment, and to hide its hydrophobic residues in its core.

However, protein structure remains a function of 1° protein structure, and as a result some hydrophilic amino acids may be present in the hydrophobic core and vice versa. It is these unstable amino acids that detract from the stability and increase the potential energy of the protein and create the LBP which makes ligand binding the final step of protein folding.

This explains how and why a protein will adopt different conformations around different ligands, as they access different unstable amino acids and create a ligand protein complex that has different energy and stability.

A new series of non-thiazolidinedione drugs have been identified *in silico*. These novel molecules have a number of advantages which include high binding affinities (*in silico*), alternative binding modalities, and Lipinski's Rule of 5 [18] compliance.

In conclusion, this study may be considered a point of departure for further design of drug like molecules of demonstrable affinity for the PPARγ.

REFERENCES:

1. World Health Organization (2011) Diabetes. WHO Fact sheet 312. World Health Organization, Geneva, Switzerland. http://www.who.int/mediacentre/factsheets/fs312/en/.
2. Greenfield JR, Chisholm DJ. Thiazolidinediones – Mechanism of Action. Aust Prescr. 2004; 27: 67-70.
3. Werner A. L., Travaglini M.T. A review of rosiglitazone in type 2 diabetes mellitus. Pharmacotherapy. 2001, 21(9), 1082-1099.
4. Home P. D., Pocock S. J., Nielsen H. B. , Gomis R. , Hanefeld M., Jones N. P., Komajda M., McMurray J.J.V. Rosiglitazone Evaluated for Cardiovascular Outcomes — An Interim Analysis. New Engl J Med. 2007, 357, 28-38.
5. GSK. GSK regulatory update on Avandia following EMA and FDA reviews. http://www.gsk.com/media/pressreleases/2010/2010_pressrelease_10103.htm (Accessed Jan 23, 2012).
6. Katzung B. G. Basic and Clinical Pharmacology; The McGraw-Hill Companies: USA, 2004.
7. Gampe RT, Montana VG, Lambert MH, Miller AB, Bledsoe RK, Milburn MV et al. Asymmetry in the PPARγ/RXRα Crystal Structure Reveals the Molecular Basis of Heterodimerization among Nuclear Receptors. Mol Cell. 2000; 5: p.545-555.
8. Salam NK, Huang THW, Kota BP, Kim SM, Li Y, Hibbs D. Novel PPAR-gamma Agonists Identified from a Natural Product Library: A Virtual Screening, Induced FitDocking and Biological Assay Study. Chem Biol Drug Des. 2008; 71: 57-70.
9. Brown KK, Henke BR, Blanchard SG, Cobb JE, Mook R, Kaldor I, *et al*. A Novel N-Aryl Tyrosine Activator of Peroxisome Proliferator-Activated Receptor-γ Reverses the Diabetic Phenotype of the Zucker Diabetic Fatty Rat. Diabetes. 1999; 48: 1415-1422.
10. Prilusky, J. (1996), "OCA, a browser-database for protein structure/function." URL *http://oca. weizmann.ac.il* and mirrors worldwide.
11. Choudhury MAI. PPARα in peroxisome proliferation: molecular characterisation and species differences. MSc thesis. University of Nottingham; 2000.
12. Molsoft LLC. Molsoft ICM Browser; ICM group: USA, 2010.
13. Tripos. Sybyl; Tripos International: St Louis; USA, 2010.
14. Wang R, Liu L, Lai L, Tang Y. SCORE: a new empirical method for estimating the binding affinity of a protein-ligand complex. J Mol Model. 1998; 4: 379-394.
15. Accelrys Draw 4.0®. Version 4.0. Symyx Solutions, Inc. San Diego, CA, USA. URL. http://www .accelrys.com.
16. Wang R, Gao Y, Lai L. Ligbuilder: a multi-purpose program for structure-based drug design. J Mol Model. 2000; 6: 498-516.
17. Agostini M, Gurnell M, Savage DB, Wood WM, Smith AG, Rajanayagam O *et al*. Tyrosine Agonists Reverse with Dominant-Negative Mutations in Human Peroxisome Proliferator-Activated Receptor γ. Endocrin. 2004; 145(4): 1527-1538.
18. Lipinski CA, Lombardo F, Dominy BW, Feeney PJ. Experimental and Computational Approaches to Estimate Solubility and Permeability in Drug Discovery and Development Settings. Adv Drug Deliver Rev. 1997; 23: 3-25.
19. Rees DC, Congreve M, Murray CW, Carr R. Fragment Based Lead Discovery. Nat Rev. 2004; 3: 660-672.
20. Congreve M, Carr R, Murray C, Jhoti H. A 'Rule of Three' for Fragment-Based Lead Discovery? Drug Discov Today. 2003; 8(19): 876-877.
21. VCCLAB, Virtual Computational Chemistry Laboratory, http:// www.vcclab.org, 2005.

Ciantar J, Shoemake C, Mangani C, Azzopardi LM and Inglott AS: Optimisation of Tyrosine-based Lead Molecules capable of modulation of the Peroxisome Proliferator-activated Receptor Gamma. *Int J Pharm Sci Res* 2012; Vol. 3(8): 2550-2561.